ACS Catalysis

Research Article

Cite This: ACS Catal. 2018, 8, 4346−4353

pubs.acs.org/acscatalysis

Design Strategy toward Recyclable and Highly Efficient Heterogeneous Catalysts for the Hydrogenation of CO_2 to Formate

Gunniya Hariyanandam Gunasekar,[†,‡] Jeongcheol Shin,[§] Kwang-Deog Jung,[‡] Kiyoung Park,[§] and Sungho Yoon*[,†]

[†]Department of Applied Chemistry, Kookmin University, 861-1 Jeongneung-dong, Seongbuk-gu, Republic of Korea

[‡]Clean Energy Research Centre, Korea Institute of Science and Technology, P.O. Box 131, Cheongryang, Republic of Korea

[§]Department of Chemistry, Korea Advanced Institute of Science and Technology, Daejeon 34141, Republic of Korea

Supporting Information

ABSTRACT: One bottleneck in the realization of CO_2 conversion into value-added compounds is the lack of catalysts with both excellent activity and recyclability. Herein, a catalyst is designed for the hydrogenation of CO_2 to formate to boost up these features by considering the leaching pathway of previously reported heterogenized catalyst; the design strategy incorporates oxyanionic ligand(s) in the coordination sphere to provide a pathway for both preventing the deleterious interactions and assisting the heterolysis of H_2. The tailored heterogenized catalyst, [bpy-CTF-Ru(acac)$_2$]Cl, demonstrated excellent recyclability over consecutive runs with a highest turnover frequency of 22 700 h^{-1}, and produced a highest formate concentration of 1.8 M in 3 h. This work is significant in elucidating new principles for the development of industrially viable hydrogenation catalysts.

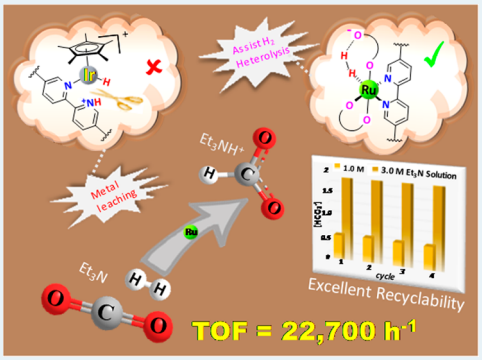

KEYWORDS: *design of hydrogenation catalyst, heterogenized CO_2 hydrogenation catalyst, oxyanionic ligated Ru complex, covalent triazine framework, formic acid production*

INTRODUCTION

Research into the mass production of value-added chemicals and fuels using the greenhouse CO_2 gas has attracted much interest over the past few decades.[1−5] To date, the commercial production of urea, carbonates, polycarbonates, and salicylic acid utilizes CO_2 as a carbon feedstock, and recently, methanol has been produced at a pilot-plant scale through CO_2 hydrogenation.[6−9] Among the multitude of CO_2 conversions reported, very few are anticipated to have the quantitative potential to reduce/consume CO_2 while providing economic benefits.[10,11] In this regard, the hydrogenation of CO_2 to formic acid/formate is one of the most promising conversions, because it offers the storage of renewable energy via H_2 in the liquid state[12,13] and produces a chemical with significant applications in various industries.[14]

During the last decades, CO_2 hydrogenation using homogeneous catalysts has been intensively investigated,[15,16] and several catalyst design approaches, including the use of proton-responsive ligands, second-coordination sphere groups, etc., have been introduced to develop the efficient homogeneous catalysts.[17−21] However, a key obstacle to the industrialization of homogeneous CO_2 hydrogenation catalysis is the separation of formic acid or formate adducts from catalyst/reaction media,[22−25] because the homogeneous catalyst present in the reaction media effectively converts the produced formic acid/formate adduct back to CO_2 and H_2 during the product isolation process. To overcome this difficulty, the use of heterogeneous catalysts is highly desirable as these catalysts can be easily secluded via simple filtration prior to the product separation step and can be continuously used for successive runs.

Accordingly, many supported/unsupported metal-nanoparticle-based heterogeneous catalysts and several heterogenized catalysts have been considered in the search for active and recyclable CO_2 hydrogenation catalysts.[23,26−37] However, the reported catalysts seriously suffer from either activity or recyclability, and the formate concentrations ([HCO_2^-]) obtained by most of these systems are remained low (see Table S1 in the Supporting Information (SI)). Hence, a potent catalyst-design strategy that provide a pathway for both enhanced catalytic activity and recyclability is currently essential to develop industrially viable heterogeneous catalysts.

Recently, we heterogenized a half-sandwich Ir-bipyridine complex on a bipyridine-based covalent triazine framework (CTF) [bpy-CTF-IrCp*Cl]Cl (Scheme 1a) for this conversion.[38] The Ir catalyst showed the best turnover frequency (TOF) of 5300 h^{-1} in the heterogeneous catalysis during the publication. However, its efficiency was decreased over consecutive runs (~10% in each cycles). A similar diminished activity upon successive runs (~12% in each cycles) was also

Received: January 29, 2018
Revised: March 27, 2018
Published: April 5, 2018

DOI: 10.1021/acscatal.8b00392
ACS Catal. 2018, 8, 4346−4353

Scheme 1. (a) Proposed Leaching Pathway for the Previously Reported [bpy-CTF-IrCp*Cl]Cl Catalyst—Deleterious Interaction between the bpy N-site and H_2, Which Causes the Leaching. (b) Plausible Design Strategy That Incorporates Oxyanionic Ligand(s) in the Coordination Sphere To Prevent the Leaching Pathway and Assist the Heterolysis of H_2. (c) Representative Structure of Oxyanionic Ligated Catalyst [bpy-CTF-Ru(acac)$_2$]Cl (1), and Its Homogeneous [Ru(bpy)(acac)$_2$]Cl (2)

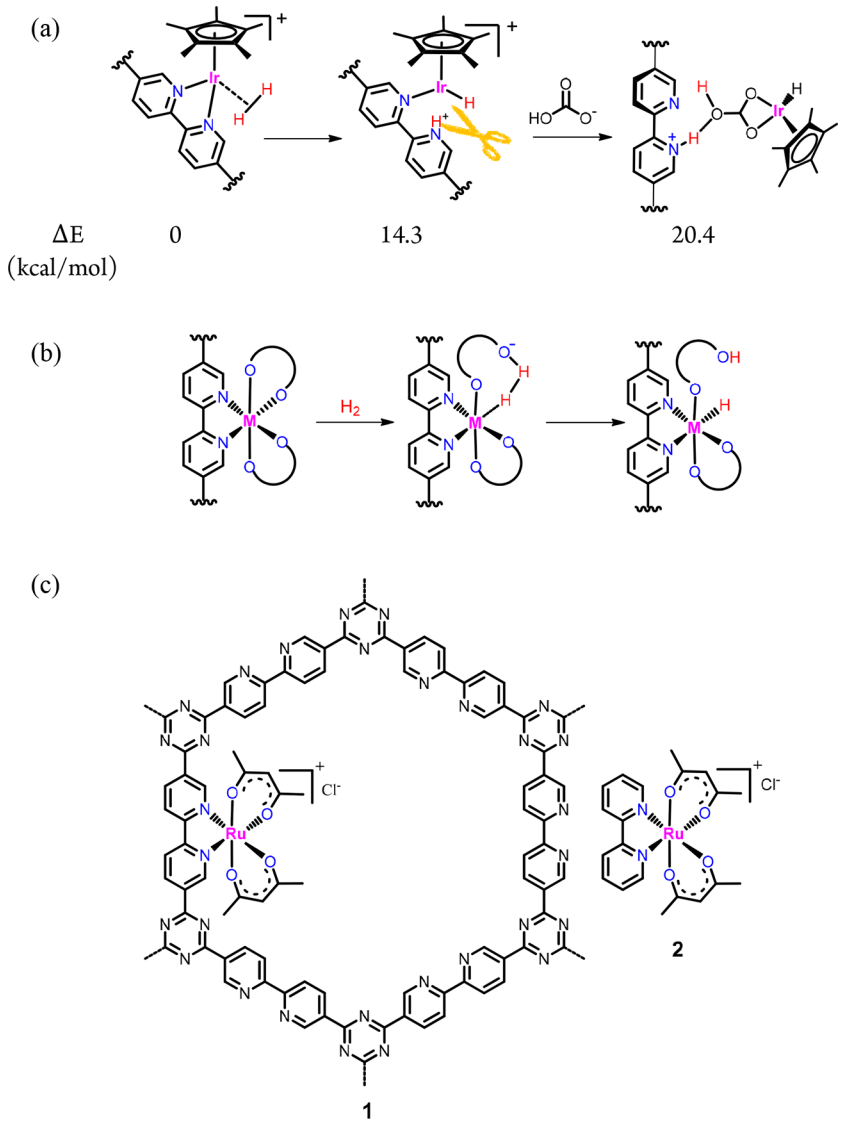

observed in the heterogenized half-sandwich Ru analogue [bpy-CTF-Ru(C_6Me_6)Cl]Cl (the detailed experimental procedure and results are discussed in the SI), suggesting that the decomposition pathway might be similar to that of the Ir catalyst. Although the homogeneous [IrCp*(bpy)Cl]Cl and [Ru(C_6Me_6)(bpy)Cl]Cl are well-known stable complexes, the decomposition/leaching was also observed in some conversions.[39]

Considering the density functional theory (DFT) study performed by Himeda et al.,[40,41] which indicated that the heterolysis of H_2 occurs via the transfer of a proton to the bicarbonate anion (HCO_3^-), the heterolysis of H_2 may occur as a minor pathway through proton transfer to the bipyridine (bpy) N-site (Scheme 1a); this may be because bpy N is always vicinal to both the metal center and the incoming H_2 molecule [the bulky half-sandwich lignads (Cp* and C_6Me_6) pushes bpy and other ligands to one side]. Consequently, the bond between the metal and bpy could dissociate and allow the metal species to leach out. To understand this, DFT calculations were performed for the Ir catalyst. The results revealed that the heterolysis of H_2 via proton transfer to the bpy N-site is feasible, given its modest uphill energy of 14.3 kcal/mol (Scheme 1a) which is reliable with the reaction temperature used (120 °C) in the experiments. With this understanding, we hypothesized that ligands such as acetylacetonate (acac), carboxylate, and HCO_3^- would be potential candidates for blocking such undesirable interaction, because the oxyanion present in the arm of the ligand (not the pyridinic N in the CTF) could rapidly abstract the proton from H_2 by changing the coordination mode from bidentate to monodentate and thus form the metal-hydride complex in a desired pathway (Scheme 1b). In addition, catalysts having such ligands would be more efficient, since they assist the heterolysis of H_2, a step that is considered as the rate-determining step for this conversion.[40,41] Hence, the introduction of oxyanionic ligand(s) in the coordination sphere would intercept the proton transfer to the ligated bpy site and simultaneously facilitate the heterolysis of H_2.

DOI: 10.1021/acscatal.8b00392
ACS Catal. 2018, 8, 4346−4353

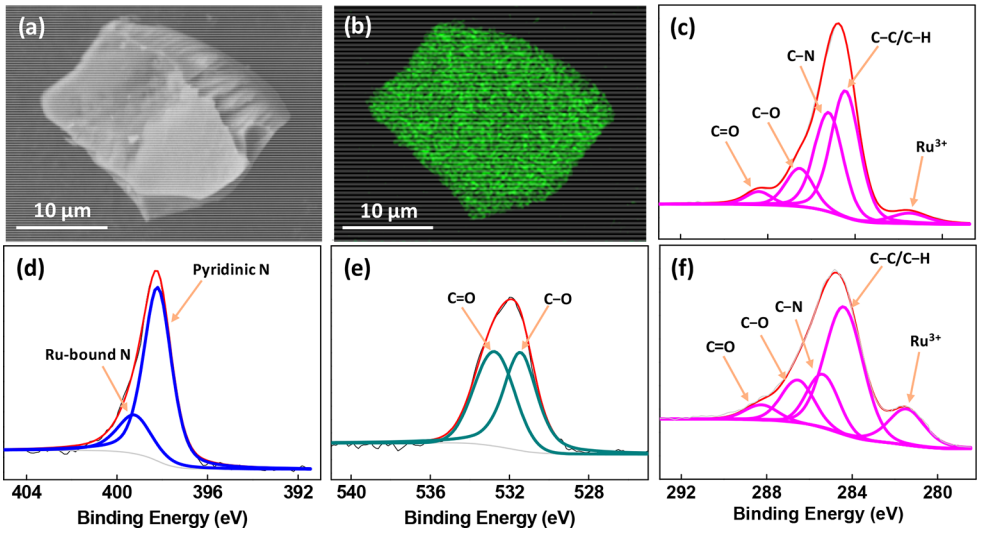

Figure 1. (a) SEM image of **1**; (b) EDS mapping of the Ru atoms in **1**. Deconvoluted XPS of **1** (c) C 1s and Ru 3d, (d) N 1s and (e) O 1s core levels; and (f) C 1s and Ru 3d core level of **2**.

The hydrogenation of CO_2 to formate using homogeneous Ru complexes is well-known and in most non-half-sandwich complexes, Ru showed higher activity than its Ir counterpart, and ligands such as acetate, acac, and phosphine (PPh_3, triphos) have been studied in this regard.[42−47] Therefore, we envisioned incorporating acac species in the Ru-bound bpy-CTF (Scheme 1c) for developing a highly robust and industrially viable catalytic entity for the hydrogenation.

Herein, we report a novel, recyclable, and highly efficient catalyst [bpy-CTF-Ru(acac)$_2$]Cl for the hydrogenation of CO_2 to formate. Catalyst **1** exhibited an unprecedented initial TOF of 22 700 h^{-1} and a turnover number (TON) of 21 200 at 120 °C under a total pressure of 8 MPa, and generated a maximum final [HCO_2^-] of 1.8 M in a short reaction time (3 h). Furthermore, as designed, this catalyst demonstrated excellent recyclability over consecutive runs.

RESULTS AND DISCUSSION

Synthesis and Characterization. A porous bpy-incorporated CTF (bpy-CTF) was synthesized by polymerizing 5,5′-dicyano-2,2′-bipyridine in $ZnCl_2$ at 400 °C.[38,48,49] The designed catalyst [bpy-CTF-Ru(acac)$_2$]Cl (**1**) (Scheme 1c), which incorporated acac ligands in the coordination sphere, was synthesized through the metalation of bpy-CTF with a Ru precursor via the following homogeneous [Ru(bpy)(acac)$_2$]Cl (**2**) synthesis.[50,51] Briefly, a suspension of bpy-CTF in methanol was stirred with $RuCl_3$ under N_2 atmosphere, and the resulting solid was treated with 2,4-pentanedione to obtain complex **1** as a robust black solid. Complex **1** is stable in air and insoluble in nearly all common organic solvents and water.

Scanning electron microscopy (SEM) and energy-dispersive spectroscopy (EDS) mapping showed that the block-shaped irregular morphology of complex **1** (with a mean size of >30(5) μm) was evenly distributed with N, O, Cl, and Ru atoms (see Figures 1a and 1b, as well as Figure S2 in the SI), indicating uniform metalation throughout the CTF matrix. The Ru:Cl ratio was 1:1, which implied the formation of complex **1**, as expected (see Table S2 in the SI). Elemental analysis revealed that the carbon content in **1** increased compared to bpy-CTF support, suggesting the presence of acac species in the framework (Table S3 in the SI). Fourier transform infrared (FT-IR) spectrum of complex **1** showed that the peak for Ru-bound carbonyl species (−C−O···Ru-), which exhibited at 1519 cm^{-1} in complex **2**, was overlapped with the broad signal of triazine species (Figure S3 in the SI). Inductively coupled plasma optical emission spectrometry (ICP-OES) analysis revealed that Ru species was loaded onto CTF at 1.68 wt %. X-ray photoelectron spectroscopy (XPS) was performed to examine the coordination environment of Ru ions. As shown in Figure 1c, the C 1s and Ru 3d core level XPS spectrum of **1** was deconvoluted into five peaks. The peak at a binding energy of 281.4 eV for the Ru $3d_{5/2}$ level demonstrated that the oxidation state of Ru in **1** is +3 (the peak for the Ru $3d_{3/2}$ level overlapped with the C−N species binding energy of 285.5 eV).[52] The peaks at 284.6, 285.2, 286.5, and 288.4 eV indicated the presence of C−C/C−H, C−N, C−O, and C═O species.[52−55] The deconvoluted N 1s spectrum had peaks at 398.2 and 399.2 eV (see Figure 1d); the peak at 398.2 eV corresponded to pyridinic N species, and the peak at 399.2 eV corresponded to metal-bound N species.[56] Similarly, the O-1*s* deconvoluted peaks at 531.4 and 532.7 eV indicated that **1** contained two types of oxygen species, i.e., C−O and C═O, respectively (Figure 1e).[57] To confirm the coordination environment of Ru ions, the XPS of **2** was compared. As shown in Figure 1f, the binding energy of Ru ion in **2** (281.4 eV) corresponded to that of **1**, reiterating the similarity in the coordination environments of Ru in both complexes.

Finally, the textural parameters of **1**, such as surface area and total pore volume, were analyzed by performing N_2 adsorption−desorption measurements at 77 K. The material exhibited both microporous and mesoporous structures similar to that of bpy-CTF (Figure S4 in the SI). However, compared to the bpy-CTF,[38] its surface area, estimated using the Brunauer−Emmett−Teller model, and total pore volume were reduced from 684 m^2/g to 502 m^2/g and from 0.40 cm^3/g to 0.29 cm^3/g, respectively. This result, coupled with XPS studies, indicated the partial occupancy of {[Ru-(acac)$_2$Cl]} units on the pore surfaces of bpy-CTF. Notably, the pores with large surface areas in complex **1** are expected to allow the smooth diffusion of small molecules such as CO_2, H_2, and H_2O during catalysis.

DOI: 10.1021/acscatal.8b00392
ACS Catal. 2018, 8, 4346−4353

Table 1. Catalytic Activity of 1[a]

entry	temperature (°C)	total pressure[b] (MPa)	[Et_3N] (M)	time, t (h)	[HCO_2^-] (M)	turnover number,[c] TON
1	90	4	1	2	0.06 (10)	720
2	100	4	1	2	0.160 (20)	1920
3	120	4	1	2	0.420 (16)	5050
4	140	4	1	2	0.290 (17)	3490
5	120	6	1	2	0.510 (10)	6140
6	120	8	1	2	0.580 (14)	6980 (22 700)[d]
7	120	8	1	5	0.580 (22)	6980
8	120	8	2	2	0.900 (13)	10 830
9	120	8	2	5	1.230 (14)	14 800
10	120	8	2	10	1.290 (17)	15 520
11	120	8	3	5	1.780 (14)	21 200
12	120	8	3	10	1.770 (16)	21 180
13[e]	120	8	3	3	1.790 (17)	2150
14[f]	120	8		20	0.0020 (5)	300
15[g]	120	8	1	20	0.0060 (8)	900

[a]Reaction conditions: 0.083 mM of **1** in an aqueous Et_3N solution (20.0 mL). [b]Total pressure at room temperature (CO_2/H_2 = 1). [c]Turnover number, which is defined as TON = moles of formate/moles of Ru. [d]Initial TOF; calculated from the initial part of the reaction (after 15 min). [e]0.831 mM of **1**. [f]Neat Et_3N solution. [g]Solvent = tetrahydrofuran (THF).

Catalytic Hydrogenation of CO_2 to Formate. The hydrogenation of CO_2 is performed in a basic aqueous solution to overcome thermodynamic barriers (see eqs S1−S3 in the SI).[58] Thus, the hydrogenation catalyzed by **1** was systematically investigated under various reaction conditions (Table 1); initially, this investigation was performed in a 1 M aqueous triethylamine (Et_3N) solution. The production of formate at various temperatures was screened at a total pressure of 4 MPa. As shown in entries 1−3 in Table 1, [HCO_2^-] gradually increased with temperature and reached a maximum of 0.42 M at 120 °C with a TON of 5050. Further increases in the temperature (140 °C) resulted in a decrease of [HCO_2^-] (entry 4 in Table 1); this might be attributed to the exothermicity of the reaction. Then, the hydrogenation was monitored at different pressure ranges; [HCO_2^-] increased with total pressure and a [HCO_2^-] of 0.58 M was obtained under 8 MPa with a TON of 6980 (entries 3, 5, and 6 in Table 1). Under the optimized temperature and pressure conditions, catalyst **1** exhibited an unprecedented initial TOF of 22 700 h^{-1} (entry 6 in Table 1), which is the best TOF value reported in the literature for this heterogeneous hydrogenation[26−36] and is ∼10 times higher than the heterogenized half-sandwich Ru catalyst, [bpy-CTF-Ru(C_6Me_6)Cl]Cl (see the SI). This indicates that the incorporation of oxyanionic ligands can significantly improve the efficiency of CO_2 hydrogenation catalysts as hypothesized.

As shown in entries 6 and 7 in Table 1, the generation of formate in a 1 M solution of Et_3N was saturated at 0.58 M, indicating that the reaction has reached chemical equilibrium; a similar remark was observed previously.[38,59] Consequently, hydrogenation was performed using different concentrations of the Et_3N solution. In a 2 M Et_3N solution, a [HCO_2^-] of 0.90 M was achieved in 2 h (entry 8 in Table 1), which then increased to 1.23 M over 5 h and reached equilibrium at this point (entries 9 and 10 in Table 1). At the same time, a [HCO_2^-] of 1.78 M (35.6 mmol) was achieved in a 3 M aqueous Et_3N solution (entries 11 and 12 in Table 1). Notably, the highest TON of 21 200 was observed during this time. Finally, to generate this high [HCO_2^-] in a short reaction time, the feeding amount of **1** was increased to 0.831 mM, and a final [HCO_2^-] of 1.79 M was obtained within just 3 h (entry 13 in Table 1).

It is noteworthy that, upon hydrogenation in the absence of water, i.e., in a neat Et_3N solution or in the nonaqueous solvents such as tetrahydrofuran (THF) (entries 14 and 15 in Table 1), the reaction rate was significantly reduced, indicating that water plays a crucial role in the performance of **1** (this is discussed later in the Theoretical Studies section).

Heterogeneity and Recycling Studies. To investigate whether catalyst **1** is actually working in a heterogeneous manner, the solid catalyst was filtered over a reaction duration of 15 min (for which a [HCO_2^-] of 0.47 M was observed in the filtrate); the resulting colorless filtrate was used as the catalytic solution. Even after an extended period of time, no increase in [HCO_2^-] was observed (Figure S5 in the SI), whereas the original reaction had a tendency to produce a [HCO_2^-] of 0.58 M in 2 h. This result suggests that catalyst **1** works in a purely heterogeneous fashion.

To demonstrate the excellent recyclability of prepared oxyanionic ligated complex, the use of **1** over multiple runs was studied. For this, the hydrogenation was initially performed in a 1 M aqueous Et_3N solution at 120 °C under a total pressure of 8 MPa for 2 h. After the initial run, the catalyst was separated by simple filtration, washed thoroughly with water, and dried under vacuum for 6 h. The dried catalyst was then directly used for the next run with a fresh 1 M Et_3N solution. As shown in Figure 2, **1** showed excellent recyclability over consecutive cycles; moreover, a total of 6.4 g of formate adduct (44.0 mmol) was obtained. Furthermore, to be industrially viable, the catalyst should also demonstrate good reusability in a highly basic Et_3N solution. Accordingly, the efficiency of **1** in the 3 M aqueous Et_3N solution over consecutive cycles was excellently maintained (Figure 2); a total of 20.5 g of formate adduct (140.0 mmol) over four cycles was generated. Hence, all these results reiterate that the introduction of oxyanionic ligand(s) in the coordination sphere remarkably enhances both reusability and activity of the hydrogenation catalysts.

SEM-EDS mapping of the recovered catalyst confirmed that the uniform distribution of Ru ions is maintained throughout the matrix (see Figure S6 in the SI). XPS analysis of the recovered catalyst revealed that the oxidation state of Ru

DOI: 10.1021/acscatal.8b00392
ACS Catal. 2018, 8, 4346−4353

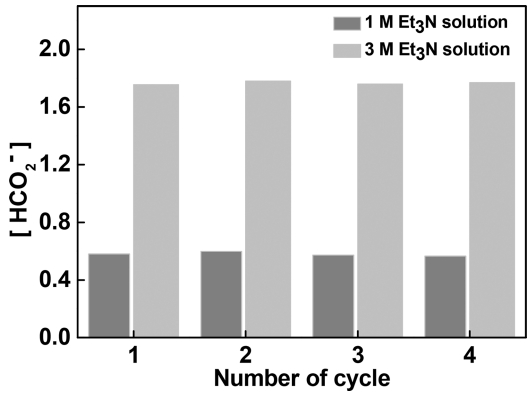

Figure 2. Recyclability of catalyst **1** at 120 °C under a total pressure of 8 MPa.

species (i.e., +3) was identical to that of fresh catalyst (Figure S7a in the SI). However, the intensity of the C−O species in the C 1s and Ru 3d spectra was partially decreased. Surprisingly, a new peak at 533.5 eV, which corresponds to metal-bound H−O−C = O species,[60] was observed in the O 1s spectrum (Figure S7b in the SI). These results may indicate that the coordination environment around the Ru(III) cation was altered, suggesting that **1** acted as a precatalyst and that the real active species formed in situ. However, the coordination adopted by Ru in the active species has not yet been completely identified, and further studies are required to determine the structure of the active species.

Theoretical Studies. To validate the design strategy and understand the mechanistic details, DFT calculations were performed (see Figure 3). The pathway involves the following two steps: (1) the formation of a metal−hydride intermediate from the reaction between H_2 and the catalyst metal center and (2) the generation of formate by the nucleophilic attack of the metal hydride on CO_2. The direct reaction between H_2 and **1** involves a change in the coordination mode of the acac ligand

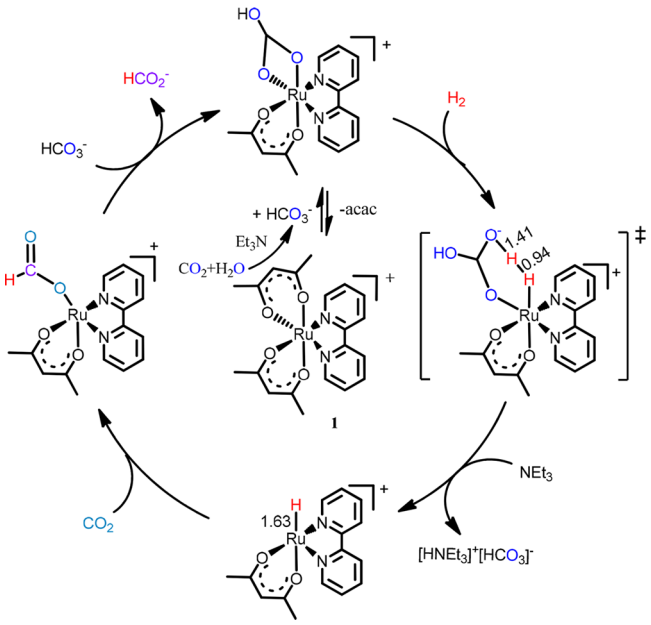

Figure 3. Proposed mechanism for the hydrogenation of CO_2 to formate, using complex **1**. Computed free energies are indicated in units of kcal/mol.

from bidentate to monodentate in order to open up one of the coordinate sites to accommodate H_2. This process is endergonic (ΔG = 30.4 kcal/mol) and involves an immense energy barrier of $\Delta G^{\ddagger}$ = 47.2 kcal/mol (see Figure S8 in the SI), which does not reflect the fast reaction rate observed. Thus, **1** is considered to act as a precatalyst, as suggested above, and another active form of the Ru complex is involved in the formation of the Ru−H bond. Because of the high CO_2 pressure and the use of aqueous media, HCO_3^- is present to a significant extent in the reaction media and may replace the acac ligand of **1** during the reaction (see Figure 3). Thus, the resulting [Ru(acac)(HCO_3)(bpy)] can react with H_2 with an energy barrier of $\Delta G^{\ddagger}$ = 16.5 kcal/mol (more-detailed information is given in Figure S9 in the SI), which is consistent with the TOF observed, and form the Ru−H complex via carbonate-assisted heterolysis of H_2 through the formation of a six-membered transition state (see Figure 3). Hence, one of the most important causes for the low activity of **1** in the absence of water (entries 14 and 15 in Table 1) may be the negligible generation of bicarbonate anions. Then, the nucleophilic attack of the thus-formed Ru−H complex on CO_2 occurs exothermally (ΔG = −11.2 kcal/mol), which is consistent with the exothermicity expected from experimental results, i.e., an energy barrier of $\Delta G^{\ddagger}$ = 8.1 kcal/mol (see Figure S10 in the SI). Compared with the heterolysis of H_2, a much smaller free-energy requirement for the addition of CO_2 to the Ru−H bond indicates that Ru−H formation is the rate-determining step. Finally, the release of the formate from the Ru−formate complex completes the catalytic cycle.

CONCLUSION

In summary, the leaching pathway of previously reported [bpy-CTF-IrCp*Cl]Cl was studied using DFT calculations, indicating that the interaction between bpy sites and H_2 during heterolysis of H_2 causes the leaching. Therefore, a new design strategy that incorporates oxyanionic ligands in the coordination sphere is developed to both prevent the deleterious interaction and improve the activity of the catalysts. The designed catalyst, [bpy-CTF-Ru(acac)$_2$]Cl (**1**) efficiently converts CO_2 to formate by hydrogenation with a TOF of 22 700 h^{-1}, which is the highest value reported to date for a heterogeneous catalyst, and exhibits excellent recyclability over consecutive runs. The viability of designed strategy was validated by DFT calculations. Further studies will focus on the comprehensive characterization of Ru coordination in the active species and involve detailed theoretical and experimental investigation into the mechanism and kinetics of the catalysis.

EXPERIMENTAL SECTION

Materials and Methods. All chemicals purchased were of analytical grade and used without further purification, unless otherwise mentioned. Zinc chloride, ruthenium(III) chloride, triethylamine were purchased from Sigma−Aldrich. Pentane-2,4-dione was purchased from Alfa Aesar. CO_2 (99.99%) and H_2 (99.99%) were purchased from Sinyang Gas Industries. The homogeneous complex **2** was prepared according to the published procedures.[50,51]

Characterization Techniques. SEM and EDS measurements were carried out using a Model JEM-7610F system (JEOL, Ltd., Japan) that was operated at an accelerating voltage of 20.0 kV. Fourier transform infrared (FT-IR) spectroscopy measurements were performed on a Nicolet iS 50 (Thermo

DOI: 10.1021/acscatal.8b00392
ACS Catal. 2018, 8, 4346−4353

Fisher Scientific). Elemental analysis was carried out on a Vario MICRO Cube instrument. X-ray photoelectron spectroscopy (XPS) data were recorded on a Model ESCA 2000 system (VG Microtech) at a pressure of ~3 × 10^{-9} mbar, using Al Kα radiation as the excitation source ($h\nu$ = 1486.6 eV) with concentric hemispherical analyzer. Ruthenium content in complex **1** was analyzed using inductively coupled plasma optical emission spectroscopy (ICP-OES) (iCAP-Q, Thermo Fisher Scientific), using microwave-assisted acid digestion system (MARS6, CEM/U.S.A). N_2 adsorption−desorption measurements were carried out in an automated gas sorption system (Belsorp II mini, BEL Japan, Inc.) at 77 K; the samples were degassed at 200 °C for 2 h before the measurements. High-performance liquid chromatography (HPLC) was measured on a Waters Alliance 2695 (Waters Corporation) system that was equipped with an Aminex HPX-87H column and an RI detector at 50 °C using 5.00 mM H_2SO_4 solution (0.6 mL/min).

Computational Methods. All computations were performed by using the Gaussian 09 (g09) package[61] with the Becke-Perdew86 (BP86) functional[62,63] and the LANL2DZ basis set/ECP combination[64−66] for geometry optimizations and frequency calculations. For single-point calculations, the LANL2TZ basis set was used for the Ru center.[64−66] The potential energy surfaces for the Ru−H formation were constructed in two dimensions along the Ru−O (of acac or bicarbonate) bond and Ru−H_2 distances, while that for the formate formation was constructed in one dimension along the hydride−CO_2 distance. From the saddle points, transition states were searched and validated using g09 intrinsic reaction coordinate calculations.[67,68]

Synthesis of bpy-CTF. In a glovebox, 5,5′-dicyano-2,2′-bipyridine[38] (1.00 g, 4.80 mmol) (see the SI for the synthesis) and zinc chloride (3.33 g, 24.0 mmol, 5 equiv) were taken in a 5 mL ampule(s) and closed with vacuum adapters. The ampule(s) was/were removed from a glovebox and sealed under vacuum, and the ampule(s) was/were heated to 400 °C in a furnace at a heating rate of 60 °C/h. After 48 h, the furnace was cooled to 200 °C at a cooling rate of 10 °C/h. The ampule was broken and the monolith was ground well in a mortar and stirred in 250 mL of water for 3 h and filtered, washed with water (600 mL) and acetone (600 mL). The resulting black solid was then refluxed in 1 M HCl (500 mL) overnight and was filtered and washed with 1 M HCl (3 × 100 mL), H_2O (3 × 100 mL), tetrahydrofuran (3 × 100 mL), and acetone (3 × 100 mL). Finally, the black powder was dried under vacuum at 200 °C for 15 h. Yield: 0.920 g.

Synthesis of Complex 1. To a solution of ruthenium(III) chloride (0.30 g, 1.44 mmol) in methanol (100 mL, anhydrous), bpy-CTF (0.500 g) was added and gently heated (60 °C) under N_2 atmosphere for 5 h and filtered. To the resulting solid, pentane-2,4-dione (3.5 mL) dissolved in H_2O:ethanol mixture (1:1) was added under N_2 atmosphere and heated for 10 h. The black solid was filtered at room temperature, washed with ethanol (3 × 500 mL), water (3 × 500 mL), and acetone (3 × 250 mL). Finally, the powder was dried under vacuum for 24 h.

Representative Procedure for the Hydrogenation of CO_2 to Formate. The hydrogenation was carried out in a 100 mL homemade stainless steel reactor equipped with a heater (temperatures up to 300 °C can be used), a burst disk pressure (which holds pressure of up to 30 MPa), and pressure and temperature sensors. In a typical run, complex **1** ([Ru] = 0.083 or 0.83 mM) was dispersed in a CO_2 saturated aqueous Et_3N solution. The reactor was tightly closed without any leak. After flushing with CO_2, the reactor was initially pressurized with CO_2 and then with H_2 (1:1) to the desired pressure at room temperature and heated at 80−140 °C. The reaction was cooled to room temperature after an appropriate time and the pressure was slowly released. The concentration of formate was analyzed by HPLC.

In the recycling experiments, the catalyst was recovered after each cycle by filtration, washed with water and acetone, and dried under vacuum before next run. By following the similar procedure, the solid was then used for successive runs.

■ ASSOCIATED CONTENT

Supporting Information

The Supporting Information is available free of charge on the ACS Publications website at DOI: 10.1021/acscatal.8b00392.

Details of the synthetic procedure and analytical data of presented CTF (PDF)

■ AUTHOR INFORMATION

Corresponding Author

*E-mail: yoona@kookmin.ac.kr.

ORCID

Sungho Yoon: 0000-0003-4521-2958

Notes

The authors declare no competing financial interest.

■ ACKNOWLEDGMENTS

We acknowledge the financial support provided by the Korea CCS R&D Center (KCRC) grant funded by the Korea government (Ministry of Science, ICT & Future Planning) (no. 2014M1A8A1049300), and C1 Gas Refinery Program through the National Research Foundation of Korea (NRF) funded by Ministry of Science and ICT (n0. 2018M3D3A1A01018006).

■ REFERENCES

(1) Centi, G.; Quadrelli, E. A.; Perathoner, S. Catalysis for CO_2 conversion: a key technology for rapid introduction of renewable energy in the value chain of chemical industries. *Energy Environ. Sci.* **2013**, *6*, 1711−1731.

(2) Sakakura, T.; Choi, J. C.; Yasuda, H. C. Transformation of Carbon Dioxide. *Chem. Rev.* **2007**, *107*, 2365−2387.

(3) Sivanesan, D.; Choi, Y.; Lee, J.; Youn, M. H.; Park, K. T.; Grace, A. N.; Kim, H.-J.; Jeong, S. K. Carbon Dioxide Sequestration by Using a Model Carbonic Anhydrase Complex in Tertiary Amine Medium. *ChemSusChem* **2015**, *8*, 3977−3982.

(4) Lin, S.; Diercks, C. S.; Zhang, Y.; Kornienko, N.; Nichols, E. M.; Zhao, Y.; Paris, A. R.; Kim, D.; Yang, P.; Yaghi, O. M.; Chang, C. J. Covalent organic frameworks comprising cobalt porphyrins for catalytic CO_2 reduction in water. *Science* **2015**, *349*, 1208−1213.

(5) Diercks, C. S.; Lin, S.; Kornienko, N.; Kapustin, E. A.; Nichols, E. M.; Zhu, C.; Zhao, Y.; Chang, C. J.; Yaghi, O. M. Reticular Electronic Tuning of Porphyrin Active Sites in Covalent Organic Frameworks for Electrocatalytic Carbon Dioxide Reduction. *J. Am. Chem. Soc.* **2018**, *140*, 1116−1122.

(6) Mikkelsen, M.; Jorgensen, M.; Krebs, F. C. The teraton challenge. *Energy Environ. Sci.* **2010**, *3*, 43−81.

(7) Goeppert, A.; Czaun, M.; Jones, J.-P.; Surya Prakash, G. K.; Olah, G. A. Recycling of carbon dioxide to methanol and derived products−closing the loop. *Chem. Soc. Rev.* **2014**, *43*, 7995−8048.

(8) Quadrelli, E. A.; Centi, G.; Duplan, J.-L.; Perathoner, S. Carbon dioxide recycling: emerging large-scale technologies with industrial potential. *ChemSusChem* **2011**, *4*, 1194−1215.

DOI: 10.1021/acscatal.8b00392
ACS Catal. 2018, 8, 4346−4353

(9) Aresta, M.; Dibenedetto, A.; Angelini, A. Catalysis for the Valorization of Exhaust Carbon: from CO_2 to Chemicals, Materials, and Fuels. Technological Use of CO_2. *Chem. Rev.* **2014**, *114*, 1709−1742.
(10) Otto, A.; Grube, T.; Schiebahn, S.; Stolten, D. Closing the loop: captured CO_2 as a feedstock in the chemical industry. *Energy Environ. Sci.* **2015**, *8*, 3283−3297.
(11) von der Assen, N.; Voll, P.; Peters, M.; Bardow, A. Life cycle assessment of CO_2 capture and utilization: a tutorial review. *Chem. Soc. Rev.* **2014**, *43*, 7982−7994.
(12) Reutemann, W.; Kieczka, H. Formic acid. In *Ullmann's Encyclopedia of Industrial Chemistry*; Wiley−VCH: Weinheim, Germany, 2011.
(13) Grasemann, M.; Laurenczy, G. Formic acid as a hydrogen source − recent developments and future trends. *Energy Environ. Sci.* **2012**, *5*, 8171−8181.
(14) Jiang, H.-L.; Singh, S. K.; Yan, J.-M.; Zhang, X.-B.; Xu, Q. Liquid-Phase Chemical Hydrogen Storage: Catalytic Hydrogen Generation under Ambient Conditions. *ChemSusChem* **2010**, *3*, 541−549.
(15) Wang, W.-H.; Himeda, Y.; Muckerman, J. T.; Manbeck, G. F.; Fujita, E. CO_2 Hydrogenation to Formate and Methanol as an Alternative to Photo- and Electrochemical CO_2 Reduction. *Chem. Rev.* **2015**, *115*, 12936−12973.
(16) Gunasekar, G. H.; Yoon, Y.; Baek, I.; Yoon, S. Catalytic reactivity of an iridium complex with a proton responsive N-donor ligand in CO_2 hydrogenation to formate. *RSC Adv.* **2018**, *8*, 1346−1350.
(17) Wang, W.-H.; Hull, J. F.; Muckerman, J. T.; Fujita, E.; Himeda, Y. Second-coordination-sphere and electronic effects enhance iridium-(III)-catalyzed homogeneous hydrogenation of carbon dioxide in water near ambient temperature and pressure. *Energy Environ. Sci.* **2012**, *5*, 7923−7926.
(18) Maenaka, Y.; Suenobu, T.; Fukuzumi, S. Catalytic interconversion between hydrogen and formic acid at ambient temperature and pressure. *Energy Environ. Sci.* **2012**, *5*, 7360−7367.
(19) Schmeier, T. J.; Dobereiner, G. E.; Crabtree, R. H.; Hazari, N. Secondary Coordination Sphere Interactions Facilitate the Insertion Step in an Iridium(III) CO_2 Reduction Catalyst. *J. Am. Chem. Soc.* **2011**, *133*, 9274−9277.
(20) Bays, J. T.; Priyadarshani, N.; Jeletic, M. S.; Hulley, E. B.; Miller, D. L.; Linehan, J. C.; Shaw, W. J. The Influence of the Second and Outer Coordination Spheres on $Rh(diphosphine)_2$ CO_2 Hydrogenation Catalysts. *ACS Catal.* **2014**, *4*, 3663−3670.
(21) Bielinski, E. A.; Lagaditis, P. O.; Zhang, Y.; Mercado, B. Q.; Wü rtele, C.; Bernskoetter, W. H.; Hazari, N.; Schneider, S. Lewis Acid-Assisted Formic Acid Dehydrogenation Using a Pincer-Supported Iron Catalyst. *J. Am. Chem. Soc.* **2014**, *136*, 10234−10237.
(22) Schaub, T.; Fries, D. M.; Paciello, R. A.; Mohl, K.-D.; Schäfer, M.; Rittinger, S.; Schneider, D. Process for preparing formic acid by reaction of carbon dioxide with hydrogen. U.S. Patent 8791297B2, 2014.
(23) Preti, D.; Squarcialupi, S.; Fachinetti, G. Production of $HCOOH/NEt_3$ Adducts by CO_2/H_2 Incorporation into Neat NEt_3. *Angew. Chem., Int. Ed.* **2010**, *49*, 2581−2584.
(24) Schaub, T.; Paciello, R. A. A Process for the Synthesis of Formic Acid by CO_2 Hydrogenation: Thermodynamic Aspects and the Role of CO. *Angew. Chem., Int. Ed.* **2011**, *50*, 7278−7282.
(25) Scott, M.; Blas Molinos, B.; Westhues, C.; Francio, G.; Leitner, W. Aqueous Biphasic Systems for the Synthesis of Formates by Catalytic CO_2 Hydrogenation: Integrated Reaction and Catalyst Separation for CO_2-Scrubbing Solutions. *ChemSusChem* **2017**, *10*, 1085−1093.
(26) Gunasekar, G. H.; Park, K.; Jung, K. D.; Yoon, S. Recent developments in the catalytic hydrogenation of CO_2 to formic acid/formate using heterogeneous catalysts. *Inorg. Chem. Front.* **2016**, *3*, 882−895.
(27) Álvarez, A.; Bansode, A.; Urakawa, A.; Bavykina, A. V.; Wezendonk, T. A.; Makkee, M.; Gascon, J.; Kapteijn, F. Challenges in the Greener Production of Formates/Formic Acid, Methanol, and DME by Heterogeneously Catalyzed CO_2 Hydrogenation Processes. *Chem. Rev.* **2017**, *117*, 9804−9838.
(28) Gunniya Hariyanandam, G.; Hyun, D.; Natarajan, P.; Jung, K. D.; Yoon, S. An effective heterogeneous Ir(III) catalyst, immobilized on a heptazine-based organic framework, for the hydrogenation of CO_2 to formate. *Catal. Today* **2016**, *265*, 52−55.
(29) Filonenko, G. A.; Vrijburg, W. L.; Hensen, E. J. M.; Pidko, E. A. On the activity of supported Au catalysts in the liquid phase hydrogenation of CO2 to formates. *J. Catal.* **2016**, *343*, 97−105.
(30) Zhang, Y.; Fei, J.; Yu, Y.; Zheng, X. 30. Silica immobilized ruthenium catalyst used for carbon dioxide hydrogenation to formic acid (I): the effect of functionalizing group and additive on the catalyst performance. *Catal. Commun.* **2004**, *5*, 643−646.
(31) Xu, Z.; McNamara, N. D.; Neumann, G. T.; Schneider, W. F.; Hicks, J. C. Catalytic Hydrogenation of CO_2 to Formic Acid with Silica-Tethered Iridium Catalysts. *ChemCatChem* **2013**, *5*, 1769−1771.
(32) Jiang, J.; Gunasekar, G. H.; Park, S.; Kim, S.-H.; Yoon, S.; Piao, L. Hierarchical Cu nanoparticle-aggregated cages with high catalytic activity for reduction of 4-nitrophenol and carbon dioxide. *Mater. Res. Bull.* **2018**, *100*, 184−190.
(33) Bavykina, A. V.; Rozhko, E.; Goesten, M. G.; Wezendonk, T.; Seoane, B.; Kapteijn, F.; Makkee, M.; Gascon, J. Shaping Covalent Triazine Frameworks for the Hydrogenation of Carbon Dioxide to Formic Acid. *ChemCatChem* **2016**, *8*, 2217−2221.
(34) Gunasekar, G. H.; Park, K.; Ganesan, V.; Lee, K.; Kim, N.-J.; Jung, K.-D.; Yoon, S. A Covalent Triazine Framework, Functionalized with Ir/N-Heterocyclic Carbene Sites, for the Efficient Hydrogenation of CO_2 to Formate. *Chem. Mater.* **2017**, *29*, 6740−6748.
(35) Su, J.; Lu, M.; Lin, H. High yield production of formate by hydrogenating CO_2 derived ammonium carbamate/carbonate at room temperature. *Green Chem.* **2015**, *17*, 2769−2773.
(36) Bi, Q.-Y.; Lin, J.-D.; Liu, Y.-M.; Du, X.-L.; Wang, J.-Q.; He, H.-Y.; Cao, Y. An Aqueous Rechargeable Formate-Based Hydrogen Battery Driven by Heterogeneous Pd Catalysis. *Angew. Chem., Int. Ed.* **2014**, *53*, 13583−13587.
(37) Su, J.; Yang, L.; Lu, M.; Lin, H. Highly Efficient Hydrogen Storage System Based on Ammonium Bicarbonate/Formate Redox Equilibrium over Palladium Nanocatalysts. *ChemSusChem* **2015**, *8*, 813−816.
(38) Park, K.; Gunasekar, G. H.; Prakash, N.; Jung, K. D.; Yoon, S. A Highly Efficient Heterogenized Iridium Complex for the Catalytic Hydrogenation of Carbon Dioxide to Formate. *ChemSusChem* **2015**, *8*, 3410−3413.
(39) Campos, J.; Hintermair, U.; Brewster, T. P.; Takase, M. K.; Crabtree, R. H. Catalyst Activation by Loss of Cyclopentadienyl Ligands in Hydrogen Transfer Catalysis with Cp*IrIII Complexes. *ACS Catal.* **2014**, *4*, 973−985.
(40) Suna, Y.; Ertem, M. Z.; Wang, W.-H.; Kambayashi, H.; Manaka, Y.; Muckerman, J. T.; Fujita, E.; Himeda, Y. Positional Effects of Hydroxy Groups on Catalytic Activity of Proton-Responsive Half-Sandwich Cp*Iridium(III) Complexes. *Organometallics* **2014**, *33*, 6519−6530.
(41) Ertem, M. Z.; Himeda, Y.; Fujita, E.; Muckerman, J. T. Interconversion of Formic Acid and Carbon Dioxide by Proton-Responsive, Half-Sandwich Cp*IrIII Complexes: A Computational Mechanistic Investigation. *ACS Catal.* **2016**, *6*, 600−609.
(42) Jessop, P. G.; Hsiao, Y.; Ikariya, T.; Noyori, R. Homogeneous Catalysis in Supercritical Fluids: Hydrogenation of Supercritical Carbon Dioxide to Formic Acid, Alkyl Formates, and Formamides. *J. Am. Chem. Soc.* **1996**, *118*, 344−355.
(43) Kothandaraman, J.; Goeppert, A.; Czaun, M.; Olah, G. A.; Surya Prakash, G. K. CO2 Capture by Amines in Aqueous Media and its Subsequent Conversion to Formate With Reusable Ruthenium and Iron Catalysts. *Green Chem.* **2016**, *18*, 5831−5838.
(44) Filonenko, G. A.; van Putten, R.; Schulpen, E. N.; Hensen, E. J. M.; Pidko, E. A. Highly Efficient Reversible Hydrogenation of Carbon Dioxide to Formates Using a Ruthenium PNP-Pincer Catalyst. *ChemCatChem* **2014**, *6*, 1526−1530.

DOI: 10.1021/acscatal.8b00392
ACS Catal. 2018, 8, 4346−4353

(45) Bosquain, S. S.; Dorcier, A.; Dyson, P. J.; Erlandsson, M.; Gonsalvi, L.; Laurenczy, G.; Peruzzini, M. Aqueous phase carbon dioxide and bicarbonate hydrogenation catalyzed by cyclopentadienyl ruthenium complexes. *Appl. Organomet. Chem.* **2007**, *21*, 947−951.
(46) Rohmann, K.; Kothe, J.; Haenel, M. W.; Englert, U.; Holscher, M.; Leitner, W. Hydrogenation of CO_2 to Formic Acid with a Highly Active Ruthenium Acriphos Complex in DMSO and DMSO/Water. *Angew. Chem., Int. Ed.* **2016**, *55*, 8966−8969.
(47) Behr, A.; Nowakowski, K. Catalytic Hydrogenation of Carbon Dioxide to Formic acid. *Adv. Inorg. Chem.* **2014**, *66*, 223−258.
(48) Sudakar, P.; Gunasekar, G. H.; Baek, I.; Yoon, S. Recyclable and Efficient Heterogenized Rh and Ir Catalysts for the Transfer Hydrogenation of Carbonyl Compounds in Aqueous Medium. *Green Chem.* **2016**, *18*, 6456−6461.
(49) Rajendiran, S.; Natarajan, P.; Yoon, S. A Covalent Triazine Framework-based Heterogenized Al−Co Bimetallic Catalyst for the Ring-expansion Carbonylation of Epoxide to β-lactone. *RSC Adv.* **2017**, *7*, 4635−4638.
(50) Payra, P.; Dutta, P. K. Development of a dissolved oxygen sensor using tris(bipyridyl) ruthenium(II) complexes entrapped in highly siliceous zeolites. *Microporous Mesoporous Mater.* **2003**, *64*, 109−118.
(51) El-Hendawy, A. M.; Alqaradawi, S. Y.; Al-Madfa, H. A. Ruthenium(III) mono (2,2′-bipyridine) complexes containing O,O-donor ligands and their oxidation properties for organic compounds. *Transition Met. Chem. (Dordrecht, Neth.)* **2000**, *25*, 572−578.
(52) Wang, F.; Xu, Q.; Tan, Z.; Li, L.; Li, S.; Hou, X.; Sun, G.; Tu, X.; Hou, J.; Li, Y. Efficient polymer solar cells with a solution-processed and thermal annealing-free RuO_2 anode buffer layer. *J. Mater. Chem. A* **2014**, *2*, 1318−1324.
(53) Huang, Y. L.; Tien, H. W.; Ma, C.-C. M.; Yang, S. Y.; Wu, S. Y.; Liu, H. Y.; Mai, Y. W. Effect of extended polymer chains on properties of transparent graphene nanosheets conductive film. *J. Mater. Chem.* **2011**, *21*, 18236−18241.
(54) Ren, L.; Yang, F.; Wang, C.; Li, Y.; Liu, H.; Tu, Z.; Zhang, L.; Liu, Z.; Gao, J.; Xu, C. Plasma synthesis of oxidized graphene foam supporting Pd nanoparticles as a new catalyst for one-pot synthesis of dibenzyls. *RSC Adv.* **2014**, *4*, 63048−63054.
(55) Permatasari, F. A.; Aimon, A. H.; Iskandar, F.; Ogi, T.; Okuyama, K. Role of C−N Configurations in the Photoluminescence of Graphene Quantum Dots Synthesized by a Hydrothermal Route. *Sci. Rep.* **2016**, *6*, 21042.
(56) Soorholtz, M.; Jones, L. C.; Samuelis, D.; Weidenthaler, C.; White, R. J.; Titirici, M.-M.; Cullen, D. A.; Zimmermann, T.; Antonietti, M.; Maier, J.; Palkovits, R.; Chmelka, B. F.; Schüth, F. Local Platinum Environments in a Solid Analogue of the Molecular Periana Catalyst. *ACS Catal.* **2016**, *6*, 2332−2340.
(57) Bagri, A.; Mattevi, C.; Acik, M.; Chabal, Y. J.; Chhowalla, M.; Shenoy, V. B. Structural evolution during the reduction of chemically derived graphene oxide. *Nat. Chem.* **2010**, *2*, 581−587.
(58) Jessop, P. G.; Ikariya, T.; Noyori, R. Homogeneous Hydrogenation of Carbon Dioxide. *Chem. Rev.* **1995**, *95*, 259−272.
(59) Himeda, Y. Conversion of CO_2 into Formate by Homogeneously Catalyzed Hydrogenation in Water: Tuning Catalytic Activity and Water Solubility through the Acid−Base Equilibrium of the Ligand. *Eur. J. Inorg. Chem.* **2007**, *2007*, 3927−3941.
(60) Zhang, L.; Li, Y.; Zhang, L.; Li, D.-W.; Karpuzov, D.; Long, Y. T. Electrocatalytic Oxidation of NADH on Graphene Oxide and Reduced Graphene Oxide Modified Screen-Printed Electrode. *Int. J. Electrochem. Sci.* **2011**, *6*, 819−829.
(61) Frisch, M. J.; Trucks, G. W.; Schlegel, H. B.; Scuseria, G. E.; Robb, M. A.; Cheeseman, J. R.; Scalmani, G.; Barone, V.; Mennucci, B.; Petersson, G. A.; Nakatsuji, H.; Caricato, M.; Li, X.; Hratchian, H. P.; Izmaylov, A. F.; Bloino, J.; Zheng, G.; Sonnenberg, J. L.; Hada, M.; Ehara, M.; Toyota, K.; Fukuda, R.; Hasegawa, J.; Ishida, M.; Nakajima, T.; Honda, Y.; Kitao, O.; Nakai, H.; Vreven, T.; Montgomery, J. A., Jr.; Peralta, J. E.; Ogliaro, F.; Bearpark, M.; Heyd, J. J.; Brothers, E.; Kudin, K. N.; Staroverov, V. N.; Kobayashi, R.; Normand, J.; Raghavachari, K.; Rendell, A.; Burant, J. C.; Iyengar, S. S.; Tomasi, J.; Cossi, M.; Rega, N.; Millam, J. M.; Klene, M.; Knox, J. E.; Cross, J. B.; Bakken, V.; Adamo, C.; Jaramillo, J.; Gomperts, R.; Stratmann, R. E.; Yazyev, O.; Austin, A. J.; Cammi, R.; Pomelli, C.; Ochterski, J. W.; Martin, R. L.; Morokuma, K.; Zakrzewski, V. G.; Voth, G. A.; Salvador, P.; Dannenberg, J. J.; Dapprich, S.; Daniels, A. D.; Farkas, O.; Foresman, J. B.; Ortiz, J. V.; Cioslowski, J.; Fox, D. J. *Gaussian 09, Revision A.1*; Gaussian, Inc.; Wallingford, CT, 2009.
(62) Becke, A. D. Density-functional exchange-energy approximation with correct asymptotic behavior. *Phys. Rev. A: At., Mol., Opt. Phys.* **1988**, *38*, 3098−3100.
(63) Perdew, J. P. Density-functional approximation for the correlation energy of the inhomogeneous electron gas. *Phys. Rev. B: Condens. Matter Mater. Phys.* **1986**, *33*, 8822−8824.
(64) Hay, P. J.; Wadt, W. R. Ab initio effective core potentials for molecular calculations. Potentials for K to Au including the outermost core orbitals. *J. Chem. Phys.* **1985**, *82*, 299−310.
(65) Hay, P. J.; Wadt, W. R. Ab initio effective core potentials for molecular calculations. Potentials for the transition metal atoms Sc to Hg. *J. Chem. Phys.* **1985**, *82*, 270−283.
(66) Wadt, W. R.; Hay, P. J. Ab initio effective core potentials for molecular calculations. Potentials for main group elements Na to Bi. *J. Chem. Phys.* **1985**, *82*, 284−298.
(67) Fukui, K. The path of chemical reactions - the IRC approach. *Acc. Chem. Res.* **1981**, *14*, 363−368.
(68) Hratchian, H. P.; Schlegel, H. B. *Theory and Applications of Computational Chemistry: The First 40 Years*; Elsevier: Amsterdam, 2005.

DOI: 10.1021/acscatal.8b00392
ACS Catal. 2018, 8, 4346−4353